Available online at www.sciencedirect.com
ScienceDirect
Combustion and Flame 153 (2008) 202–215
Combustion and Flame
www.elsevier.com/locate/combustflame

Sensitivity calculations in PDF particle methods

Zhuyin Ren *, Stephen B. Pope

Sibley School of Mechanical and Aerospace Engineering, Cornell University, Ithaca, NY 14853, USA

Received 30 April 2007; received in revised form 25 October 2007; accepted 29 October 2007

Available online 3 March 2008

Abstract

In combustion modeling, it is desirable to know how sensitive the predictions are to certain parameters in the model formulation. In this study, we develop a method for accurate and efficient sensitivity calculation in PDF modeling of turbulent combustion. This method enables the calculation of the sensitivities for each particle in PDF particle methods. These particle-level sensitivities are very revealing. They allow one to examine the particles with the largest sensitivities, and the corresponding compositions reveal the sensitive region of composition space. By ensemble averaging the particle sensitivities, sensitivities of mean (and conditional mean) quantities can be extracted. The method is applied to the PDF calculations of the oxidation of diluted hydrogen in a partially stirred reactor (PaSR) using three different mixing models. It is demonstrated that the method is capable of accurately calculating the sensitivities at the particle level. The study also illustrates the qualitatively different behavior of the three mixing models as revealed by both the particle composition and the particle sensitivities. The sensitivities of mean (and conditional mean) quantities reveal the controlling processes in a PaSR. They confirm that when combustion is controlled by mixing, the combustion is insensitive to chemistry; when the system is close to global extinction, the combustion is extremely sensitive both to mixing and to chemistry.

Keywords: Sensitivity analysis; In situ adaptive tabulation; Particle-level sensitivities; PDF methods

1. Introduction

Modeling combustion phenomena requires the knowledge of chemical kinetics, transport properties, turbulence/combustion model parameters, etc. as input parameters, and produces predictions (such as species concentration profiles, flame speed, etc.) as the output, with the input and the output connected by the governing model equations. Often it is desirable to know how sensitive the predictions are to certain parameters in the model formulation. Sensitivity analysis is a formal approach to examine quantitatively the relationship between the parameters and the output of the model. Since it was introduced to combustion research, it has been widely used in understanding and improving chemical kinetic models, in uncertainty analysis, and in gaining insight into the model performance. Examples of the application of sensitivity analysis in chemical kinetics and laminar flames can be found in [1–9]. For example, sensitivity analyses have been performed on elementary reaction rates. Thus, without solving the problem repetitively with different values for the rate constants, sensitivity analysis allows one to understand how the model responds to changes in the rate parameters. It also provides insight about how important certain reaction pathways are to the model's predictions.

* Corresponding author. Fax: +1 607 255 1222.
E-mail address: zr26@cornell.edu (Z. Ren).

0010-2180/$ – see front matter
doi:10.1016/j.combustflame.2007.10.017

In the fields of chemical kinetics and laminar flames, tools and softwares for sensitivity analysis are well developed. For example, a series of computer codes (e.g., SENKIN [10], CHEMKIN [11], CANTERA [12]) have been developed. These codes have been used as a routine procedure in kinetic modeling and sensitivity analysis for homogeneous gas phase reactions.

For turbulent combustion calculations, it would be equally valuable to perform sensitivity analysis, but the tools are less well developed. For example, in modeling turbulent reactive flows based on PDF methods [13], it is valuable to know the sensitivity of the predictions to the mixing model constant as well as to other parameters. In the past, somewhat crude analyses have been performed to evaluate sensitivities by repeating a calculation with a single parameter changed by a small amount. This divided difference technique has been used to show the strong sensitivity of some PDF calculations of turbulent flames to the temperature of a pilot stream [14,15], to a reaction rate [16], and to the mixing model constant C_ϕ governing the rate of turbulent mixing [14,17–19]. However, using divided differences in the Monte Carlo methods used to solve the PDF equations is costly and inefficient, as the statistical errors need to be reduced so as to be small compared to the differences in the two calculations.

In this study, we develop a method for the accurate and efficient calculation of sensitivities in PDF modeling of turbulent combustion. This method is demonstrated in the PDF calculation of a partially stirred reactor (PaSR) burning a hydrogen–air mixture with three different mixing models: interaction by exchange with the mean (IEM or LMSE) model [20,21]; the modified Curl mixing (MC) model [22]; and the Euclidean minimum spanning tree (EMST) model [23,24]. With the IEM model, accurate sensitivities can be obtained by other means and hence can be used to validate the accuracy of the method.

The remainder of the paper progresses as follows. In Section 2, the mathematical formulation of the sensitivity calculation in PDF particle methods is outlined. In Section 3, the sensitivity calculations in a PaSR are described. Results and comparisons are shown in Section 4. Conclusions are drawn in Section 5.

2. Formulation

2.1. Sensitivity equation

In a PDF calculation of a reactive flow involving n_s species, with the Monte Carlo techniques [13], the distribution of compositions is represented by an ensemble of N particles. The composition $\boldsymbol{\phi}^{(n)}$ of the nth particle consists of the n_s species-specific moles (denoted by $\mathbf{z}$, kmol/kg, mass fractions divided by the corresponding species molecular weights) and enthalpy, i.e., $n_\phi = n_\mathrm{s} + 1$ quantities. In the PDF calculation, the change in particle composition due to reaction is treated exactly, while molecular mixing is represented by mixing models (e.g., IEM, MC, EMST) which prescribe the evolution of the particles in composition space such that they mimic the change in the composition of a fluid particle due to molecular mixing in a turbulent reactive flow. We consider a set $\mathbf{a} = \{a_1, a_2, \ldots, a_{n_\mathrm{a}}\}$ of n_a sensitivity parameters. These could be the temperature of an inflowing stream; a species mass fraction in an inflowing stream; a pre-exponential factor or an activation energy in a reaction rate; or the mixing model constant. In a fuller notation, $\phi_i^{(n)}(t;\mathbf{a})$ denotes the ith composition of the nth particle at time t for a PDF calculation performed with the sensitivity parameters having the values $\mathbf{a}$. The $n_\phi \times n_\mathrm{a}$ sensitivity matrix $\mathbf{W}^{(n)}(t;\mathbf{a})$ (for the nth particle at time t) is then defined by

$$W_{ij}^{(n)}(t;\mathbf{a}) \equiv \frac{\partial \phi_i^{(n)}(t;\mathbf{a})}{\partial a_j}. \tag{1}$$

In general, in the PDF calculation of a reactive flow, the evolution equation for $\boldsymbol{\phi}^{(n)}(t;\mathbf{a})$ is given by

$$\frac{d\phi_i^{(n)}(t;\mathbf{a})}{dt} = S_i\big(\boldsymbol{\phi}^{(n)}(t;\mathbf{a});\mathbf{a}\big) + C_\phi M^{(n)}\big(\{\phi_i(t;\mathbf{a})\}\big), \tag{2}$$

where $\mathbf{S}$ is the rate of change due to chemical reactions, C_ϕ is the mixing model constant, and $M^{(n)}$ denotes the effect of the mixing model, which depends on the ensemble $\{\boldsymbol{\phi}\}$ of particle compositions. For the IEM model we have

$$M^{(n)}\big(\{\phi_i(t;\mathbf{a})\}\big) = \frac{1}{2\tau_\mathrm{t}}\big(\tilde{\phi}_i - \phi_i^{(n)}\big), \tag{3}$$

where $\tilde{\boldsymbol{\phi}}$ is the Favre mean composition (i.e., the ensemble average of particle compositions $\{\boldsymbol{\phi}\}$) and τ_t is the characteristic turbulence time scale. To compute the sensitivity matrix $\mathbf{W}^{(n)}(t;\mathbf{a})$ for each particle, we make the following assumptions:

- We neglect the change in density $\rho^{(n)}(t)$ due to changes in the parameters, i.e., we assume that $\partial\rho^{(n)}(t)/\partial a_j$ is negligible. Hence the velocity and turbulence fields are (by assumption) independent of infinitesimal changes in $\mathbf{a}$.
- We neglect nonlinear effects in the mixing models. The IEM (see Eq. (3)) and MC mixing models are linear in the composition, as is the under-

lying physics. In the MC model, particle composition evolves by processes that are linear in the composition (see [22] for more details).

The EMST model is a more complicated particle-interaction model, where the change in particle composition is determined by particle interactions along the edges of a Euclidean minimum spanning tree constructed on the ensemble of particles in composition space. In the model, after the construction of the EMST, the particle composition evolves according to a set of linear equations (see [23] for more details). However, the construction of the EMST is based on the composition, which involves nonlinear operations. In this regard, the EMST model is nonlinear. The assumption, then, is that the topology of the EMST (i.e., the construction of the EMST) is unaffected by infinitesimal changes in $\mathbf{a}$.

With the above assumptions, differentiating Eq. (2) with respect to a_j, we obtain the following evolution equation for the sensitivities $\mathbf{W}^{(n)}(t;\mathbf{a})$:

$$\frac{dW_{ij}^{(n)}}{dt} = J_{ik}^{(n)} W_{kj}^{(n)} + V_{ij}^{(n)} + \frac{\partial C_\phi}{\partial a_j} M^{(n)}\big(\{\phi_i\}\big) + C_\phi M^{(n)}\big(\{W_{ij}\}\big), \tag{4}$$

where the summation convention applies and $\mathbf{J}^{(n)}$ is the $n_\phi \times n_\phi$ Jacobian matrix

$$J_{ij} \equiv \frac{\partial S_i(\boldsymbol{\phi};\mathbf{a})}{\partial \phi_j}, \tag{5}$$

and V_{ij} is the sensitivity of the reaction source term to $\mathbf{a}$

$$V_{ij} \equiv \frac{\partial S_i(\boldsymbol{\phi};\mathbf{a})}{\partial a_j}. \tag{6}$$

In Eq. (4), the last two terms represent the effect of mixing on particle sensitivities, which depend on the ensemble $\{\boldsymbol{\phi}\}$ of particle compositions and the ensemble $\{\mathbf{W}\}$ of particle sensitivities, respectively. In general, the matrices $\mathbf{J}$ and $\mathbf{V}$ in Eq. (4) can be accurately and efficiently evaluated using automatic differentiation (e.g., by using ADIFOR [25]). (For special cases, analytical expressions can be obtained for $\mathbf{J}$ and $\mathbf{V}$.)

In the computational implementation of the method, for the nth particle, the sensitivity matrix $\mathbf{W}^{(n)}(t)$ is represented (in addition to the composition $\boldsymbol{\phi}^{(n)}(t)$), which can result in a significant increase in storage requirements (i.e., by a factor of n_a). The particle properties $\boldsymbol{\phi}^{(n)}(t)$ and $\mathbf{W}^{(n)}(t)$ then evolve by Eqs. (2) and (4) with appropriate initial and boundary conditions. If a_j is a model parameter, then the appropriate boundary condition is $W_{ij} = 0$. But if a_j corresponds to the value of ϕ_i on the boundary considered, then the boundary condition is $W_{ij} = 1$.

One thing worth mentioning is that the above formulation enables sensitivity calculation for each particle. These particle-level sensitivities are very revealing. For example, in a region of significant local extinction in turbulent combustion, they allow one to examine the particles with the largest sensitivities, and the corresponding compositions reveal the sensitive region in the composition space. Moreover, sensitivities of mean (and conditional mean) quantities can be extracted by ensemble averaging the particle sensitivities.

Notice that the sensitivity parameters and the various output quantities of the combustion model may have different units; for example, rate coefficients belonging to reactions of different orders have different units. In such cases, the elements of the sensitivity matrix $\mathbf{W}$ are incomparable. The results are most easily understood in terms of normalized sensitivities, such as the nondimensional logarithmic sensitivities

$$\tilde{W}_{ij}^{(n)}(t;\mathbf{a}) \equiv \frac{a_j}{\phi_i^n(t;\mathbf{a})} \frac{\partial \phi_i^{(n)}(t;\mathbf{a})}{\partial a_j} = \frac{a_j}{\phi_i^n} W_{ij}^{(n)}(t;\mathbf{a}) \tag{7}$$

and the dimensional semilogarithmic sensitivities

$$\hat{W}_{ij}^{(n)}(t;\mathbf{a}) \equiv a_j \frac{\partial \phi_i^{(n)}(t;\mathbf{a})}{\partial a_j} = a_j W_{ij}^{(n)}(t;\mathbf{a}), \tag{8}$$

where the summation convention does not apply. The logarithmic sensitivity $\tilde{W}_{ij}$ represents the fractional change in composition $\phi_i^{(n)}$ caused by an infinitesimal fractional change of the parameter a_j.

2.2. Splitting scheme

The evolution equations for the particle composition, Eq. (2), and the particle sensitivities, Eq. (4), can be accurately integrated by numerical schemes based on an operator-splitting approach [26,27]. These schemes split the governing equation into subequations, with each having a single operator capturing only a portion of the physics present, and then they time integrate each separately and sequentially to advance to the next time step. Equations (2) and (4) can be advanced from t over a time step Δt to $t + \Delta t$ through a Strang splitting scheme [28] as follows:

(1) Substep 1. We consider the reaction source terms. The system to be solved (written in a simplified matrix notation) over a time step $\Delta t/2$ is

$$\frac{d\boldsymbol{\phi}^{(n)}}{dt} = \mathbf{S}\big(\boldsymbol{\phi}^{(n)}\big), \tag{9}$$

$$\frac{d\mathbf{W}^{(n)}}{dt} = \mathbf{J}\big(\boldsymbol{\phi}^{(n)}\big)\mathbf{W}^{(n)} + \mathbf{V}\big(\boldsymbol{\phi}^{(n)}\big). \tag{10}$$

The initial conditions for $\boldsymbol{\phi}^{(n)}$ and $\mathbf{W}^{(n)}$ are taken to be the final state from the previous time step. At the completion of this substep, the final state of the system serves as the initial conditions for the next substep. In this study, we directly solve Eqs. (9) and (10) using the ODE solver DDASAC [29]. The direct integration of Eqs. (9) and (10) for each particle at each time step in the PDF calculation of real turbulent flames is computationally inefficient and costly. An efficient alternative for solving Eqs. (9) and (10) is to use a storage–retrieval method such as in situ adaptive tabulation (ISAT) [30]. The efficient solution for Eqs. (9) and (10) via ISAT is discussed in Section 2.3.

(2) Substep 2. The system to be solved over a time step Δt (from t to $t+\Delta t$) is

$$\frac{d\phi_i^{(n)}}{dt} = C_\phi M^{(n)}\big(\{\phi_i\}\big),$$
$$\frac{dW_{ij}^{(n)}}{dt} = C_\phi M^{(n)}\big(\{W_{ij}\}\big) + \frac{\partial C_\phi}{\partial a_j} M^{(n)}\big(\{\phi_i\}\big). \tag{11}$$

The initial conditions for $\boldsymbol{\phi}^{(n)}$ and $\mathbf{W}^{(n)}$ are taken to be the final state from the previous substep. If the mixing model constant C_ϕ is not included as one of the sensitivity parameters, then $\partial C_\phi/\partial a_j$ is zero and the last term in the sensitivity equation is absent. For this case, the system is solved simply by applying the mixing model to each component of the particle composition and the particle sensitivities over a time step Δt. The legitimacy of this simple procedure stems from the linearity of the mixing operation. Otherwise, if C_ϕ is one of the sensitivity parameters, let $a_1 = C_\phi$, so that $\partial C_\phi/\partial a_j = \delta_{1j}$. The particle compositions and the particle sensitivities to other sensitivity parameters except C_ϕ are still obtained simply by applying the mixing model to each component of them over a time step Δt. The sensitivities to the mixing model constant C_ϕ are computed as follows.

The governing equation for the sensitivities to C_ϕ during this substep is

$$\frac{dW_{i1}^{(n)}}{dt} = C_\phi M^{(n)}\big(\{W_{i1}\}\big) + M^{(n)}\big(\{\phi_i\}\big). \tag{12}$$

A second-order accurate solution to Eq. (12) can be obtained by the following three steps:

- Substep 2(i): Integrate half of the term $M^{(n)}(\{\phi_i\})$ in Eq. (12) over a time step Δt from t to $t+\Delta t$ to yield simply

$$W_{i1}^{*(n)} = W_{i1}^{(n)}(t) + \frac{1}{2C_\phi}\int_t^{t+\Delta t} C_\phi M^{(n)}\big(\{\phi_i\}\big)\,dt = W_{i1}^{(n)}(t) + \frac{1}{2C_\phi}\big(\Delta\phi_i^{(n)}\big)_{\text{mix}}, \tag{13}$$

where $W_{i1}^{(n)}(t)$ is the final state from the previous substep (Substep 1), and $(\Delta\boldsymbol{\phi}^{(n)})_{\text{mix}}$ denotes the change in composition due to mixing in the current substep (Substep 2). (Note that the integrand in the first line of Eq. (13) is the rate of change of $\phi_i^{(n)}$ given by Eq. (11).)

- Substep 2(ii): Apply the mixing model to each component of $W_{i1}^{*(n)}$ over a time step Δt. We denote the sensitivities after mixing by $W_{i1}^{**(n)}$.
- Substep 2(iii): Integrate the other half of the term $M^{(n)}(\{\phi_i\})$ over the time step from t to $t+\Delta t$, to yield, simply,

$$W_{i1}^{(n)}(t+\Delta t) = W_{i1}^{**(n)} + \frac{1}{2C_\phi}\big(\Delta\phi_i^{(n)}\big)_{\text{mix}}. \tag{14}$$

(3) Substep 3. A substep identical to Substep 1 is performed, taking as the initial conditions the final state of the system from Substep 2. At the completion of this substep, the final state of the system is the solution at the end of the time step and serves as the initial conditions for the next time step.

As demonstrated in Section 4.1, the above splitting scheme is second-order accurate in time for both composition and sensitivities.

2.3. Efficient implementation of the reaction substep

In this section, we show how Eqs. (9) and (10) for the reaction substep can be solved efficiently using in situ adaptive tabulation (ISAT) [30]. In PDF calculations without sensitivity analysis, during the reaction substep, the governing equation is given by Eq. (9). Given the initial composition $\boldsymbol{\phi}(t_0)$ at time t_0, the reaction mapping $\boldsymbol{\phi}(t_0+\Delta t)$ after a time step Δt can be efficiently computed by the ISAT algorithm. That is, the composition $\boldsymbol{\phi}(t_0+\Delta t)$ at the end of the time step is tabulated as a function of the initial composition $\boldsymbol{\phi}(t_0)$. Table entries are added as needed (for possible later use) by using DDASAC to solve Eq. (9) for $\boldsymbol{\phi}(t_0+\Delta t)$, in conjunction with the equation

$$\frac{d\mathbf{A}(t)}{dt} = \mathbf{J}\big(\boldsymbol{\phi}(t)\big)\mathbf{A}(t), \tag{15}$$

from the initial condition $\mathbf{A}(t_0) = \mathbf{I}$ to obtain the $n_\phi \times n_\phi$ matrix of sensitivities with respect to the initial

composition. The matrix $\mathbf{A}(t_0 + \Delta t)$ is stored in the ISAT table and is used in the construction of a linear approximation for $\boldsymbol{\phi}(t_0 + \Delta t)$.

With a very simple extension, the ISAT algorithm can be used to compute the sensitivity matrix $\mathbf{W}(t_0 + \Delta t)$ efficiently. This is based on the observation that the solution to Eq. (10) can be written as

$$\mathbf{W}(t) = \mathbf{W}^0(t) + \mathbf{A}(t)\mathbf{W}(t_0), \tag{16}$$

where $\mathbf{W}(t_0)$ is the initial condition and $\mathbf{W}^0(t)$ is the solution to Eq. (10) from the initial condition $\mathbf{W}^0(t_0) = 0$. Notice that $\mathbf{W}^0(t)$ depends solely on $\boldsymbol{\phi}(t_0)$ and t. The sensitivity matrix after a time step Δt is

$$\mathbf{W}(t_0 + \Delta t) = \mathbf{W}^0(t_0 + \Delta t) + \mathbf{A}(t_0 + \Delta t)\mathbf{W}(t_0). \tag{17}$$

While $\mathbf{W}(t_0 + \Delta t)$ depends on both $\boldsymbol{\phi}(t_0)$ and $\mathbf{W}(t_0)$, a key observation is that $\mathbf{W}^0(t_0 + \Delta t)$—like $\boldsymbol{\phi}(t_0 + \Delta t)$ and $\mathbf{A}(t_0 + \Delta t)$—depends solely on $\boldsymbol{\phi}(t_0)$. Thus, when an entry is added to the ISAT table, $\mathbf{W}^0(t_0 + \Delta t)$ is computed using DDASAC and stored in the table. Then, for each particle on each time step, the appropriate values of $\mathbf{A}(t_0 + \Delta t)$ and $\mathbf{W}^0(t_0 + \Delta t)$ are retrieved from the ISAT table and $\mathbf{W}(t_0 + \Delta t)$ is evaluated by Eq. (17). The additional computational work (beyond that needed to compute $\boldsymbol{\phi}(t_0 + \Delta t)$) is simply the matrix–matrix multiplication $\mathbf{AW}$ which requires of order $n_a n_\phi^2$ operations—at most a factor of n_a more than is already required by ISAT for composition computation.

In summary, with a simple extension to ISAT, the $n_\phi \times n_a$ sensitivity matrix $\mathbf{W}$ can be efficiently computed for each particle. Both the memory and the CPU time per time step are greater by at most a factor of n_a compared to the computation without sensitivities.

3. Sensitivity calculations in a partially stirred reactor (PaSR)

To demonstrate the above method, we consider the sensitivity calculation in the PDF calculations of the oxidation of a diluted H_2/air mixture in an adiabatic PaSR. Due to its simplicity, the PaSR has been widely used to investigate combustion models and numerical algorithms [31–34]. It is similar to a single grid cell embedded in a large PDF computation of turbulent combustion.

In this study, the pressure is atmospheric throughout and the PaSR is continuously fed by two inlets, which inject cold nonpremixed fuel and oxidant into the reactor at the mass flow rates $\dot{m}_{fu}$ and $\dot{m}_{ox}$, respectively. In our simulations, the two inflow streams are the fuel stream (H_2 and N_2, γ:1 by volume, $T = 305$ K) and the oxidant stream (N_2 and O_2, 79:21 by volume, $T = 305$ K). In the calculations, the hydrogen-to-nitrogen ratio of the fuel stream is $\gamma = 1$. The inflow mass fraction of the oxidant stream, P, is defined as $P = \dot{m}_{ox}/[\dot{m}_{ox} + \dot{m}_{fu}]$. In our simulations, the inflow mixture yields stoichiometry (with stoichiometric mixture fraction $\xi_{st} = 0.304$) and therefore $P = 0.696$. The composition $\boldsymbol{\phi}$ consists of species-specific moles (kmol/kg) and enthalpy and it determines the thermochemical state of the mixture. The compositions of the inflow oxidant and fuel streams are denoted by $\boldsymbol{\phi}^0$ and $\boldsymbol{\phi}^1$, respectively. Inside the reactor, reaction occurs and the mean thermochemical properties are assumed to be statistically spatially homogeneous, but the fluid is imperfectly mixed at the molecular level. Simultaneously, the resulting mixture is withdrawn from the reactor at a rate equal to the total mass inflow rates, i.e., $\dot{m} = \dot{m}_{ox} + \dot{m}_{fu}$; hence the mass m of fluid inside the reactor is constant.

The combustion process in a PaSR is characterized by three time scales: the residence time τ_{res}, the specified turbulence time scale τ_t, and the characteristic chemical time scale τ_c. The residence time τ_{res} is defined as $\tau_{res} = m/\dot{m}$ and the chemical time scale τ_c is determined by the chemical mechanism. Here the detailed mechanism [35] for hydrogen oxidation, which involves 9 species and 19 reactions, is incorporated into the calculations. The mixing time τ_{mix}, which determines the decay of the variance of composition, is related to the turbulence time τ_t by the mixing model constant C_ϕ through $\tau_{mix} = \tau_t/C_\phi$. In the PaSR, the inflow mixtures are nonpremixed cold fuel and cold oxidant. As shown in [34], global extinction occurs for a fixed value of τ_{mix}/τ_{res} when τ_{res} is reduced to a point at which chemical reactions cannot be sustained. Also, global extinction occurs as τ_{mix} increases (for a fixed value of τ_{res}) due to insufficient mixing. In this study, we consider the first circumstance. With a fixed value of $\tau_t/\tau_{res} = 0.5$, calculations with decreasing τ_{res} are performed. In the following, we present the calculation results with $C_\phi = 2.0$, i.e., a fixed value of $\tau_{mix}/\tau_{res} = 0.25$. Qualitatively similar results are obtained (not shown) with other specifications of C_ϕ (e.g., $C_\phi = 1$ and 3), which correspond to different values of τ_{mix}/τ_{res}.

For demonstration, we consider the sensitivities of the PDF calculation to the mixing model constant C_ϕ, the hydrogen-to-nitrogen ratio of the fuel stream γ, and the pre-exponential factors for the following three chain reactions:

$$\begin{aligned} &\text{R1} \quad O_2 + H \rightleftarrows OH + O, \\ &\text{R2} \quad H_2 + O \rightleftarrows OH + H, \\ &\text{R3} \quad H_2 + OH \rightleftarrows H_2O + H. \end{aligned} \tag{18}$$

(The sensitivity to C_ϕ essentially contains the same information as the sensitivity to the mixing time $\tau_{\rm mix}$ since $\tau_{\rm mix}$ is inversely linearly proportional to C_ϕ by $\tau_{\rm mix} = \tau_{\rm t}/C_\phi$.) Hence the sensitivity parameters considered are $\mathbf{a} = \{C_\phi; \gamma; \alpha_1; \alpha_2; \alpha_3\}$, where α_1, α_2 and α_3 are the pre-exponential factors of reactions R1, R2, and R3, respectively.

The evolution equations for particle composition $\boldsymbol{\phi}^{(n)}(t;\mathbf{a})$ and particle sensitivities $\mathbf{W}^{(n)}(t;\mathbf{a})$ are given by Eqs. (2) and (4). The Jacobian matrix $\mathbf{J}$ in Eq. (4) is obtained by automatic differentiation using ADIFOR. The matrix $\mathbf{V}$ in Eq. (4) is determined as follows. The rate of change $\mathbf{S}$ can be written as a summation of the contributions from all reactions involving the ith species

$$S_i = \sum_{k=1}^{n_{\rm r}} \nu_{ik}\omega_k(\alpha_k), \tag{19}$$

where $n_{\rm r}$ is the number of elementary reactions, and α_k, ν_{ik}, and ω_k are the pre-exponential factor, the overall stoichiometric coefficients, and the overall reaction rate of the kth reaction, respectively. For the three chain reactions considered, since ω_k is linear in α_k, the sensitivities of the reaction source term to the pre-exponential factors are given by

$$\frac{\partial S_i(\boldsymbol{\phi};\mathbf{a})}{\partial \alpha_k} = \frac{1}{\alpha_k}\nu_{ik}\omega_k, \tag{20}$$

where the summation convention does not apply. The sensitivities of the reaction source term to C_ϕ and to γ are

$$\frac{\partial S_i(\boldsymbol{\phi};\mathbf{a})}{\partial C_\phi} = 0, \qquad \frac{\partial S_i(\boldsymbol{\phi};\mathbf{a})}{\partial \gamma} = 0. \tag{21}$$

In the following, we show how the particle composition and particle sensitivities are accurately solved in fractional steps. In the stochastic simulation of the PaSR based on the Monte Carlo methods, at any time t, the PaSR consists of an even number N of particles, the nth particle having composition $\boldsymbol{\phi}^{(n)}(t)$, and its age in the PaSR being denoted by $s^{(n)}(t)$. In our simulations, at any time t, the PaSR consists of an even number N of particles and each particle represents a mass m/N of fluid. With Δt being the specified time step, at the discrete times $k\Delta t$ (k integer) events occur corresponding to *inflow* and *outflow*, which can cause the particle composition $\boldsymbol{\phi}^{(n)}(t)$ and sensitivities $\mathbf{W}^{(n)}(t)$ to change discontinuously. Between these discrete times, the particle composition and sensitivities evolve by the *mixing* and *reaction* processes. The procedure for solving the *mixing* and *reaction* processes has been given in Section 2.2. The inflow/outflow is now described in more detail.

Inflow/outflow. Choose $N_{\rm replaced}(= N \times \Delta t/\tau_{\rm res})$ particles randomly with replacement from the ensemble of N particles, and replace them with an equal number of particles from the inflow streams. For the composition of the fuel stream $\boldsymbol{\phi}^1$, all the species-specific moles are zero except the specific moles of species H_2 and N_2, which are given by

$$z_{\rm H_2} = \frac{\gamma}{\gamma w_{\rm H_2} + w_{\rm N_2}},$$
$$z_{\rm N_2} = \frac{1}{\gamma w_{\rm H_2} + w_{\rm N_2}}, \tag{22}$$

where $w_{\rm H_2}$ and $w_{\rm N_2}$ are the molecular weights of species H_2 and N_2. The sensitivities (to the sensitivity parameters $\{C_\phi; \gamma; \alpha_1; \alpha_2; \alpha_3\}$) for the incoming particles are set to zero, except that for the incoming particles from the fuel stream the sensitivities of the following quantities to γ are specified as

$$\frac{\partial z_{\rm H_2}}{\partial \gamma} = \frac{w_{\rm N_2}}{(\gamma w_{\rm H_2} + w_{\rm N_2})^2},$$
$$\frac{\partial z_{\rm N_2}}{\partial \gamma} = -\frac{w_{\rm H_2}}{(\gamma w_{\rm H_2} + w_{\rm N_2})^2}, \tag{23}$$

which follows from Eq. (22).

In the calculations, at any time t, the PaSR consists of $N = 1000$ particles. The initial condition is that all particles are in chemical equilibrium with the stoichiometric mixture fraction $\xi_{\rm st}$ (= 0.304). The initial sensitivities are zero for all particles. The time step Δt is chosen to be $\frac{1}{40}\min(\tau_{\rm res}, \tau_{\rm t})$. The ODE error tolerances for DDASAC are $\varepsilon_{\rm a} = 1 \times 10^{-12}$ for absolute error and $\varepsilon_{\rm r} = 1 \times 10^{-9}$ for relative error. The numerical settings for N, Δt, $\varepsilon_{\rm a}$, and $\varepsilon_{\rm r}$ are sufficient to ensure numerical accuracy for both composition and sensitivity. In the following section, we present the results when the PaSR has reached statistical stationarity. Some of the results presented below involve conditional Favre averages. These are denoted by $\langle \bullet|\eta\rangle_\rho \equiv \langle \bullet\rho|\eta\rangle/\langle\rho|\eta\rangle$, where ρ is density and η is the sample-space variable corresponding to mixture fraction ξ. The range of ξ used to estimate the quantities conditional on the mixture being stoichiometric is from 0.254 to 0.354. In practice, $\langle \bullet|\xi_{\rm st}\rangle_\rho$ is obtained by averaging over all particles with $0.254 \leqslant \xi \leqslant 0.354$.

4. Results and discussion

In this section, we first validate the method given in Section 2 for calculating sensitivities in PDF calculations. Then we investigate and compare the sensitivities from different mixing models.

4.1. Validation of the methodology for sensitivity calculation in PDF methods

With the IEM mixing model, the evolution equation for $\phi_i^{(n)}(t;\mathbf{a})$ in the PaSR is

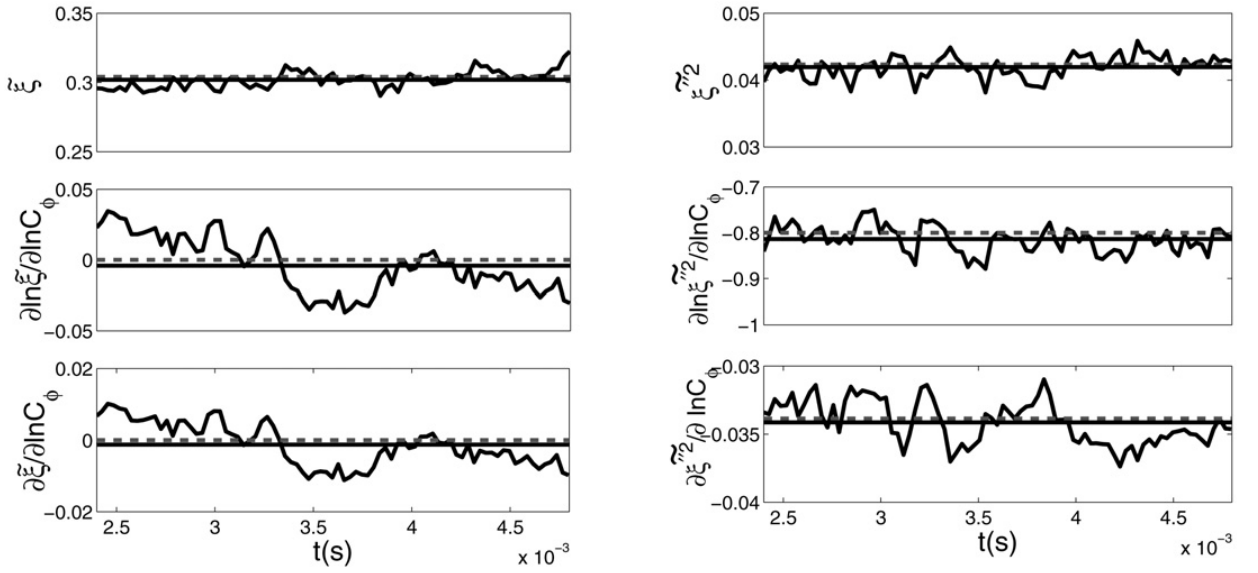

Fig. 1. Favre mean and variance of mixture fraction and their sensitivities to the mixing model constant C_ϕ for the PaSR in the statistically stationary state, with $\tau_{\rm res} = 3 \times 10^{-4}$ s and $\tau_{\rm t} = 1.5 \times 10^{-4}$ s. Black curve: instantaneous predictions from the PDF calculation; dashed line: exact values given by Eqs. (27)–(29); black line: time-averaged predictions from the PDF calculation (averaged from 0.0024 s to 0.0048 s, i.e., eight residence times).

$$\frac{d\phi_i^{(n)}}{dt} = S_i(\boldsymbol{\phi}^{(n)}; \mathbf{a}) - C_\phi \frac{\phi_i^{(n)} - \tilde{\phi}_i}{2\tau_{\rm t}}, \tag{24}$$

where $\tilde{\boldsymbol{\phi}}$ is the Favre mean composition (known from the ensemble of particle compositions $\{\boldsymbol{\phi}\}$). The corresponding evolution equation for the sensitivities is

$$\frac{dW_{ij}^{(n)}}{dt} = J_{ik}^{(n)} W_{kj}^{(n)} + \frac{\partial S_i(\boldsymbol{\phi}^{(n)}; \mathbf{a})}{\partial a_j} - \frac{\delta_{j1}(\phi_i^{(n)} - \tilde{\phi}_i)}{2\tau_{\rm t}} - C_\phi \frac{W_{ij}^{(n)} - \tilde{W}_{ij}}{2\tau_{\rm t}}, \tag{25}$$

where the summation convention applies, and $\tilde{\mathbf{W}}$ is the matrix of Favre mean sensitivities (known from the ensemble of particle sensitivities $\{\mathbf{W}\}$). With the IEM model, accurate sensitivities can be obtained by other means as shown below, and hence these accurate sensitivities can be used to validate the present method for sensitivity calculation in PDF methods.

With the IEM model, when a statistical stationary solution is reached in the PaSR, the transport equation for the PDF of mixture fraction, $\tilde{p}(\eta)$, is

$$0 = -\frac{\tilde{p}(\eta)}{\tau_{\rm res}} + \frac{1}{\tau_{\rm res}}\big[P\delta(\eta) + (1-P)\delta(1-\eta)\big] + \frac{\partial}{\partial\eta}\left[\frac{C_\phi}{2\tau_{\rm t}}(\eta - \tilde{\xi})\tilde{p}(\eta)\right]. \tag{26}$$

As shown in [34], by multiplying both sides of Eq. (26) by η and integrating from $-\infty$ to ∞, the Favre mean of mixture fraction $\tilde{\xi}$ in the statistically stationary state can be obtained as

$$\tilde{\xi} = 1 - P. \tag{27}$$

By multiplying both sides of Eq. (26) by $(\eta - \tilde{\xi})^2$ and integrating from $-\infty$ to ∞, the variance of mixture fraction $\widetilde{\xi''^2}$ in the statistically stationary state can be obtained as

$$\widetilde{\xi''^2} = \frac{P(1-P)}{1 + C_\phi \tau_{\rm res}/\tau_{\rm t}}. \tag{28}$$

Hence the sensitivities of the Favre mean and variance of mixture fraction to the mixing model constant are

$$\frac{\partial\tilde{\xi}}{\partial C_\phi} = 0, \qquad \frac{\partial\widetilde{\xi''^2}}{\partial C_\phi} = -\frac{P(1-P)\tau_{\rm res}/\tau_{\rm t}}{(1 + C_\phi\tau_{\rm res}/\tau_{\rm t})^2}. \tag{29}$$

Fig. 1 shows the exact (given by Eqs. (27)–(29) and calculated Favre mean and variance of mixture fraction and their sensitivities to the mixing model constant C_ϕ. The calculated values of $\tilde{\xi}$, $\widetilde{\xi''^2}$, and their sensitivities are extracted from the ensemble of particle compositions $\{\boldsymbol{\phi}\}$ and particle sensitivities $\{\mathbf{W}\}$ on each time step. As may be seen from the figure, the instantaneous predictions fluctuate around the exact values due to the finite number of particles used in the PDF calculation. Time averaging (over a time 2.4×10^{-3} s, or, equivalently, 640 time steps) is used to estimate the means with reduced statistical error. As may be seen from Fig. 1, the calculated means are in good agreement with the exact values. The remaining differences are caused by numerical errors such as statistical and splitting errors.

With the IEM model, when statistical stationarity is reached, the mean composition $\tilde{\boldsymbol{\phi}}$ and the mean

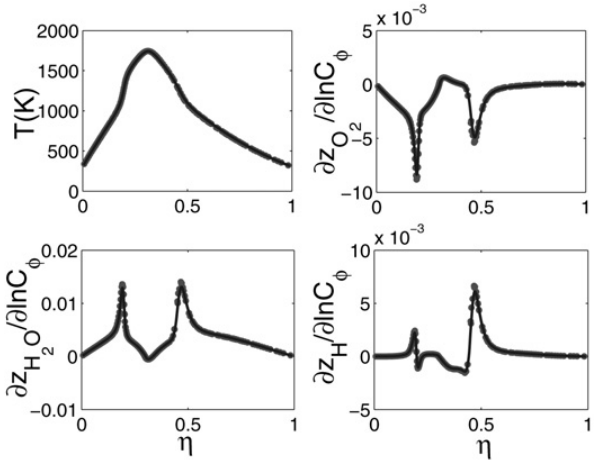

Fig. 2. Temperature and sensitivities of different species with respect to C_ϕ against mixture fraction η with $\tau_{\text{res}} = 3 \times 10^{-4}$ s and $\tau_{\text{t}} = 1.5 \times 10^{-4}$ s. Gray dots: scatterplot obtained from the PDF calculation; black line: prediction from Eqs. (24) and (25) with the initial conditions being $\boldsymbol{\phi}(t=0) = \boldsymbol{\phi}^0$ and $\mathbf{W}(t=0) = \mathbf{0}$ (or $\boldsymbol{\phi}(t=0) = \boldsymbol{\phi}^1$ and $\mathbf{W}(t=0) = \mathbf{0}$), the mean composition and sensitivities $\tilde{\boldsymbol{\phi}}$ and $\tilde{\mathbf{W}}$ being extracted from the PDF calculation.

sensitivity $\tilde{\mathbf{W}}$ are constant. Hence, with the knowledge of the air or fuel stream the particle originates from, the particle composition $\boldsymbol{\phi}^{(n)}$ and sensitivities $\mathbf{W}^{(n)}$ are unique functions of its age $s^{(n)}$ in the PaSR. With the knowledge of $\tilde{\boldsymbol{\phi}}$ and $\tilde{\mathbf{W}}$, the exact composition and sensitivities can be obtained by integrating Eqs. (24) and (25) with the initial conditions being $\{\boldsymbol{\phi}^{(n)}(t=0) = \boldsymbol{\phi}^0, \mathbf{W}^{(n)}(t=0) = \mathbf{0}\}$ or $\{\boldsymbol{\phi}^{(n)}(t=0) = \boldsymbol{\phi}^1, \mathbf{W}^{(n)}(t=0) = \mathbf{0}\}$ (depending on the air or fuel stream the particle originates from). These observations provide another, independent means of computing $\boldsymbol{\phi}^{(n)}$ and $\mathbf{W}^{(n)}$, which we use as a further test of the correctness of the method. In this study, we take approximations to $\tilde{\boldsymbol{\phi}}$ and $\tilde{\mathbf{W}}$ from the PDF calculation. (There may be small differences between the approximations and exact values of $\tilde{\boldsymbol{\phi}}$ and $\tilde{\mathbf{W}}$ due to the numerical errors in the PDF calculation.) With these approximated means, composition and sensitivities are obtained by integrating Eqs. (24) and (25). The composition and sensitivities obtained from this approach should agree well with the composition and sensitivities obtained from the PDF calculation. This is confirmed in Fig. 2, which shows the temperature and sensitivities of different species with respect to C_ϕ obtained from the two different methods. As may be seen from the figure, relative to their maximum absolute values, the maximum difference between the semilogarithmic sensitivities calculated by the two different methods is 7%. Hence the present method is capable of accurately calculating the sensitivities at the particle level. The small differences are caused by numerical errors in the PDF calculation and the error in the means $\tilde{\boldsymbol{\phi}}$ and $\tilde{\mathbf{W}}$ used in integrating Eqs. (24) and (25).

As mentioned, with the IEM model, when statistical stationarity is reached, the particle composition and sensitivities can be obtained with high accuracy by directly integrating Eqs. (24) and (25) forward in time using an ODE solver (with the mean composition and sensitivities $\tilde{\boldsymbol{\phi}}$ and $\tilde{\mathbf{W}}$ being extracted from the PDF calculation). To demonstrate the accuracy of the splitting scheme described in Section 2.2, Eqs. (24) and (25) are alternatively solved using the splitting scheme. In each of the substeps, the corresponding governing equations are solved accurately so that (over the range of Δt considered) the only significant numerical error is the splitting error. We define

$$\varepsilon_z(\Delta t) \equiv \frac{1}{\max|\mathbf{z}^{\text{DI}}(t)|} \max\left(\left|\mathbf{z}^{\text{DI}}(t) - \mathbf{z}^{\text{SP}}(t, \Delta t)\right|\right), \quad \text{for } 0 < t < t_{\text{end}}, \tag{30}$$

to be the measure of the error between the accurate species-specific moles $\mathbf{z}^{\text{DI}}(t)$ from the direct integration of the full coupled equations (Eqs. (24) and (25)), and the solution $\mathbf{z}^{\text{SP}}(t, \Delta t)$ from the splitting-scheme with time step Δt. (For the results presented below $t_{\text{end}} = 2 \times 10^{-3}$ s.) We define

$$\varepsilon_{\text{w}}(\Delta t) \equiv \frac{1}{\max|\mathbf{U}^{\text{DI}}(t)|} \max\left(\left|\mathbf{U}^{\text{DI}}(t) - \mathbf{U}^{\text{SP}}(t, \Delta t)\right|\right), \quad \text{for } 0 < t < t_{\text{end}} \tag{31}$$

(with $U_i = \partial z_i / \partial \ln C_\phi$) to be the measure of the error between the accurate sensitivities from the direct integration of Eqs. (24) and (25) and the solution from the splitting scheme with time step Δt. Fig. 3 compares the sensitivities from the direct integration and the splitting scheme with different time steps. The initial conditions are $\boldsymbol{\phi}(t=0) = \boldsymbol{\phi}^1$ and $\mathbf{W}(t=0) = \mathbf{0}$. As shown in the figure, the difference is small. Fig. 4 shows the numerical errors in both composition and sensitivities against the time step. The errors decrease with Δt, essentially as Δt^2, thus illustrating the second-order accuracy of the splitting scheme. With $\Delta t/\tau_{\text{t}} = 0.025$, the relative error incurred in the sensitivities is less than 4×10^{-4}. (Recall that in this study the time step Δt in the PDF calculations is chosen to be $0.025 \min(\tau_{\text{res}}, \tau_{\text{t}})$. For all the results shown, $\tau_{\text{res}} > \tau_{\text{t}}$.)

4.2. Sensitivities in PDF calculations with the IEM model

In mixture fraction space, Fig. 5 shows the scatter plots of particle temperature T, particle specific moles of H_2O, sensitivities of H_2O with decreasing values of τ_{res} and a fixed ratio of $\tau_{\text{t}}/\tau_{\text{res}} = 0.5$. As may be seen from the scatterplot of H_2O, for the

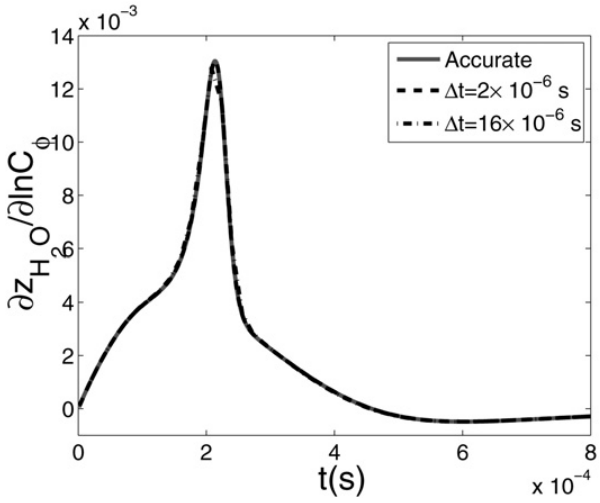

Fig. 3. Comparison between the accurate direct integration of Eqs. (24) and (25) and the splitting scheme (see Section 2.2) with different time steps. Figure showing the sensitivity of H_2O with respect to C_ϕ against time. The initial conditions are $\boldsymbol{\phi}(t=0)=\boldsymbol{\phi}^1$ and $\mathbf{W}(t=0)=\mathbf{0}$, $\tau_t = 1.5\times 10^{-4}$ s, and the mean composition and sensitivities $\tilde{\boldsymbol{\phi}}$ and $\tilde{\mathbf{W}}$ are extracted from the PDF calculation.

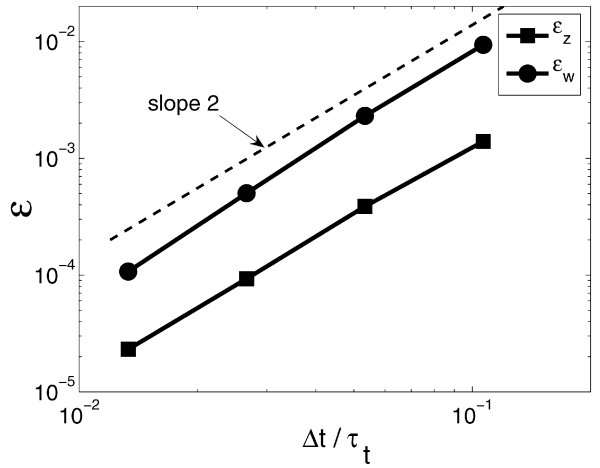

Fig. 4. Demonstration of the accuracy of the splitting scheme in Section 2.2 for solving the particle composition equation (24) and the particle sensitivities equation (25) with $\tau_t = 1.5\times 10^{-4}$ s. The initial conditions are $\boldsymbol{\phi}(t=0)=\boldsymbol{\phi}^1$ and $\mathbf{W}(t=0)=\mathbf{0}$. The mean composition and sensitivities $\tilde{\boldsymbol{\phi}}$ and $\tilde{\mathbf{W}}$ are extracted from the PDF calculation. Figure showing the splitting error in composition ε_z (defined by Eq. (30)) and the splitting error in sensitivities ε_W (defined by Eq. (31)) against time step Δt. Also shown are the dashed line of slope 2 corresponding to second-order accuracy ($\varepsilon(\Delta t)\sim\Delta t^2$).

IEM model, the evolution of particle composition is consistent with the following picture: particles corresponding to composition values outside the reaction zone relax toward the mean composition and are away from chemical equilibrium; particles in the reaction zone react back toward their equilibrium values due to reaction. The particle sensitivities depend on the corresponding composition's location in the mixture fraction space. The most sensitive region lies on the fuel-lean and fuel-rich boundaries of the reaction zone, not on the stoichiometric mixture fraction. With the decrease of residence time toward global extinction, the particle temperature and the specific moles of H_2O decrease consistently. Moreover, the fuel-lean and fuel-rich boundaries of the reaction zone move toward stoichiometry. Correspondingly, the most sensitive region in the composition space moves toward stoichiometry. Also, with the decrease of the residence time, the sensitivities both to the mixing time and to the rates of the three chain reactions increase. Another thing worth mentioning is that the shapes of the sensitivities to the rates of the three chain reactions in the composition space are similar. Similar observations can be made from the scatterplots of radicals such as OH as shown in Fig. 6. Hence, as demonstrated, the sensitivities obtained from the PDF calculations allow one to examine the particles with the largest sensitivities, and the corresponding compositions reveal the sensitive region of composition space. Also, the sensitivities allow one to study the sensitivities in the region of interest in composition space.

By ensemble averaging the particle sensitivities, sensitivities of mean quantities can be extracted. Figs. 7 shows sensitivities of mean species-specific moles against residence time. As expected, for large residence times, the mean species-specific moles are relatively insensitive to the rates of the chain reactions, i.e., insensitive to chemistry. In contrast, the system is sensitive to the mixing model constant, i.e., sensitive to mixing. With the decrease of residence time toward global extinction, sensitivities of the mean species-specific moles increase (in magnitude). This observation can also be made from the scatter plots shown in Fig. 5. When the system is close to global extinction, the combustion is sensitive both to the mixing and to the chemistry. (With the IEM model for the fixed ratio of $\tau_t/\tau_{res}=0.5$, the system extinguishes around $\tau_{res}=8\times 10^{-5}$ s.) Notice that close to global extinction, the sensitivities to the mixing are of the same order of magnitude as (but higher than) the sensitivities to the chemistry, which reveals that close to extinction mixing is still the controlling process for combustion in the PaSR with $\tau_t/\tau_{res}=0.5$. For some other values of τ_t/τ_{res} such as $\tau_t/\tau_{res}\to 0$ (not shown), the system is not sensitive to mixing; close to extinction, reaction is the controlling process and the sensitivities to chemistry dominate.

4.3. Comparison of the sensitivities between different mixing models

The method for sensitivity calculation presented here can be applied straightforwardly to PDF calculations with other mixing models such as MC and

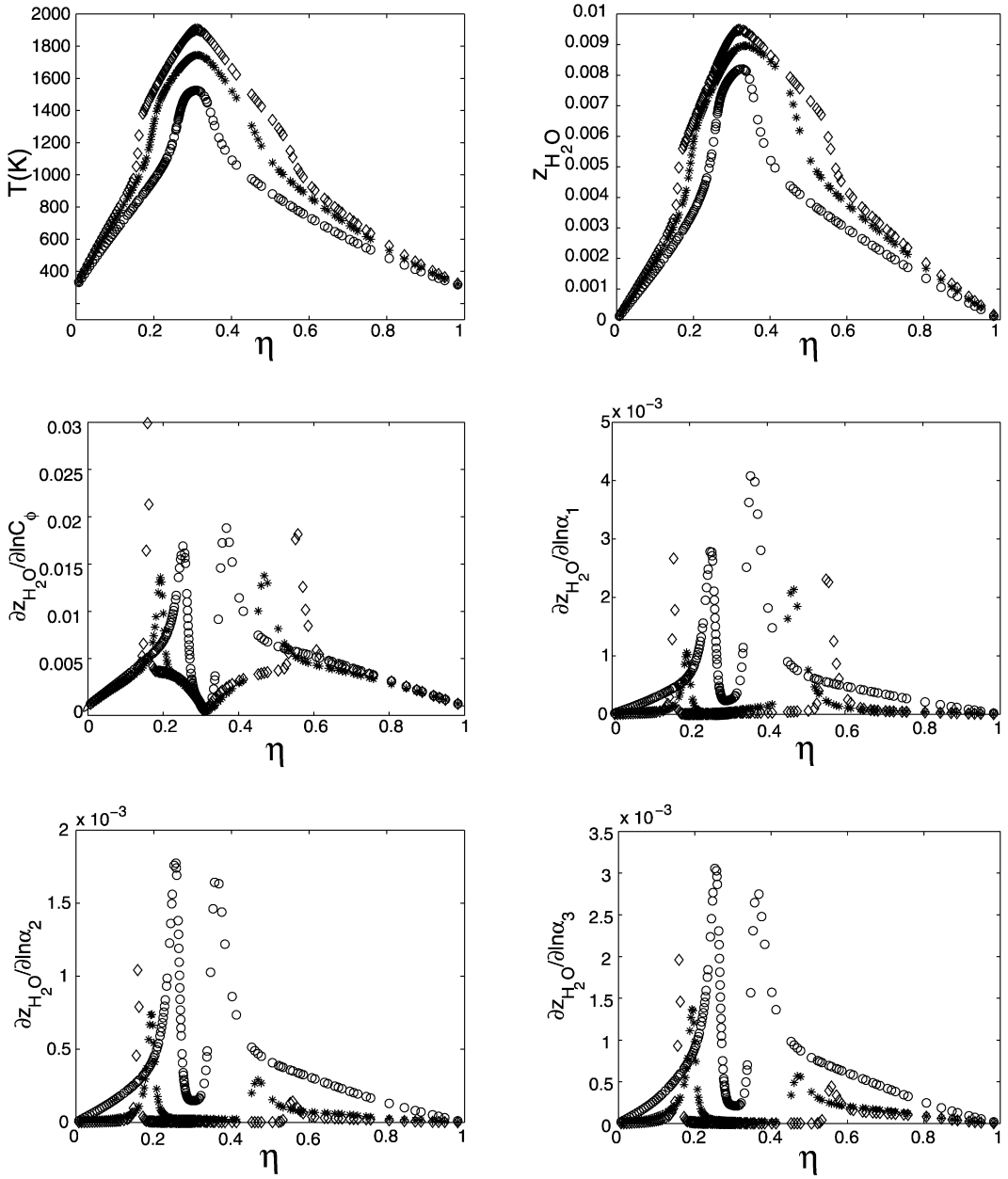

Fig. 5. For the IEM model, in the mixture fraction space, scatterplots of temperature T, species-specific moles of H_2O, sensitivities of H_2O to C_ϕ, and the pre-exponential factors of reactions listed in Eq. (18) for different values of τ_{res} with $\tau_t/\tau_{res} = 0.5$. ($\diamond$) $\tau_{res} = 2$ ms; ($*$) $\tau_{res} = 0.3$ ms; ($\circ$) $\tau_{res} = 0.08$ ms.

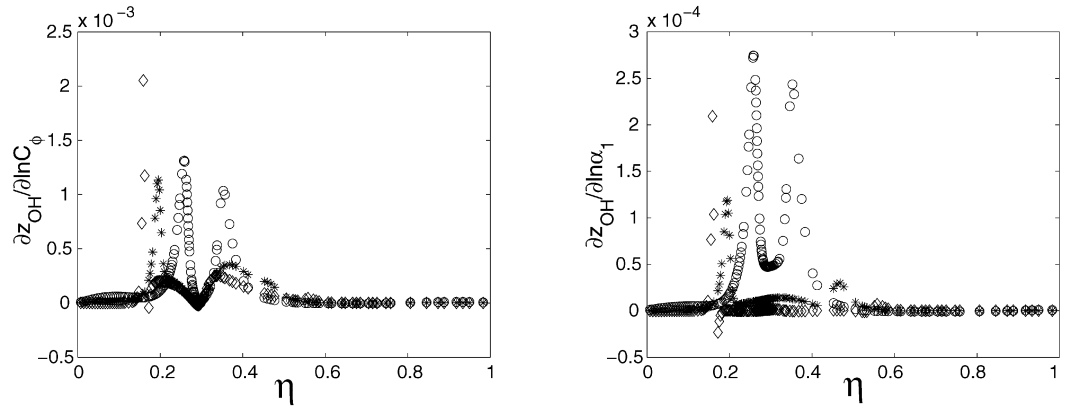

Fig. 6. For the IEM model, in the mixture fraction space, scatterplots of sensitivities of OH to C_ϕ and to the pre-exponential factor α_1 of R1 for different values of τ_{res} with $\tau_t/\tau_{res} = 0.5$. ($\diamond$) $\tau_{res} = 2$ ms; ($*$) $\tau_{res} = 0.3$ ms; ($\circ$) $\tau_{res} = 0.08$ ms.

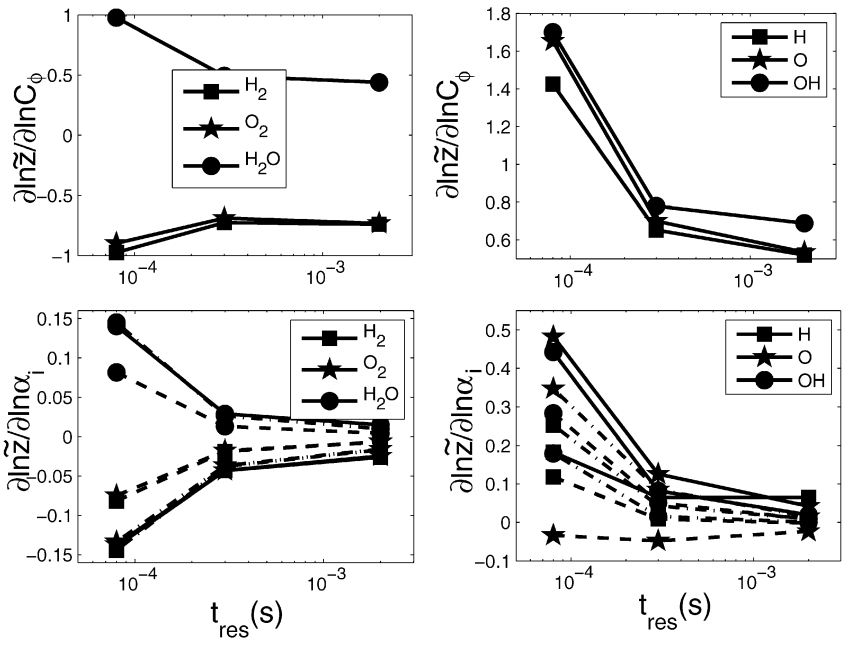

Fig. 7. Sensitivities (to the mixing model constant C_ϕ and the pre-exponential factors α_i of the reactions listed in Eq. (18)) of conditional mean species-specific moles (conditional on stoichiometric mixture fraction) against residence time with $\tau_t/\tau_{res} = 0.5$. In bottom row, solid line: sensitivities to the pre-exponential factor of R1; dashed line: sensitivities to the pre-exponential factor of R2; dashed–dotted line: sensitivities to the pre-exponential factor of R3.

EMST. As previously mentioned, for EMST some approximation is involved, since the model is nonlinear. In the mixture fraction space, Fig. 8 shows the scatterplots of temperature T, sensitivities of H_2O to the mixing model constant C_ϕ, and sensitivities of H_2O to the pre-exponential factor α_1, from different mixing models. (The sensitivities of H_2O to α_2 and α_3 are qualitatively similar to those to α_1.)

For all the mixing models, the particle sensitivities depend on their locations in mixture fraction space. However, there are qualitatively different behaviors in both the compositions and the sensitivities. For the IEM model, the most sensitive region (for both C_ϕ and α_1) lies on the boundaries of the reaction zone. With the decrease of the residence time toward global extinction, the most sensitive region in the composition space moves toward stoichiometry. In contrast, for the EMST model, both the most sensitive region and the shape of the sensitivity distribution in the composition space remain almost the same over a wide range of residence times. However the most sensitive region for the mixing parameter C_ϕ is different from that for the reaction parameter α_1. For the system considered, the most sensitive region for C_ϕ in mixture fraction space is around $\xi = 0.12$ and 0.78, not at stoichiometric composition ($\xi_{st} = 0.304$); for α_1, it is around $\xi = 0.4$, closer to stoichiometric composition. For the MC model, due to the randomness in the model, no clear pattern can be observed from these particle-level sensitivities. Nevertheless as revealed by the particle sensitivities the most sensitive region is around stoichiometric.

Qualitative differences in the mixing models can also be observed in the sensitivities to the hydrogen-to-nitrogen ratio γ of the fuel stream. (Recall that for the fuel stream, the larger the value of γ, the higher the concentration of H_2.) As shown in Fig. 9, for the IEM model, a local maximum of the sensitivities occurs at the fuel-lean boundary of the reaction zone, whereas a local minimum exists at the fuel-rich boundary. For the EMST model, the most sensitive region is around $\xi = 0.25$, which is different from those for C_ϕ and α_1. Hence for the EMST model, the most sensitive regions in the composition space are different for different parameters.

In Figs. 10 and 11, we compare the sensitivities of the mean (and conditional mean) quantities from the three mixing models. Figs. 10 and 11 show the sensitivities of H_2O against the residence time (with a fixed ratio of $\tau_t/\tau_{res} = 0.5$) till global extinction occurs. As shown, the EMST model is more resistant to global extinction than the IEM and MC models. For the three different mixing models, the sensitivities of both the mean and conditional mean specific moles of H_2O show qualitatively the same behavior: with the decrease of the residence time toward global extinction, sensitivities increase. For large residence time where combustion is controlled by the mixing process, as expected, for all the mixing models, the system is insensitive to the pre-exponential factors of the chain reactions, i.e., insensitive to chemistry. When τ_{res} is reduced close to global extinction, the sensitivities of the combustion process both to the mixing time and to the chemistry increase dramati-

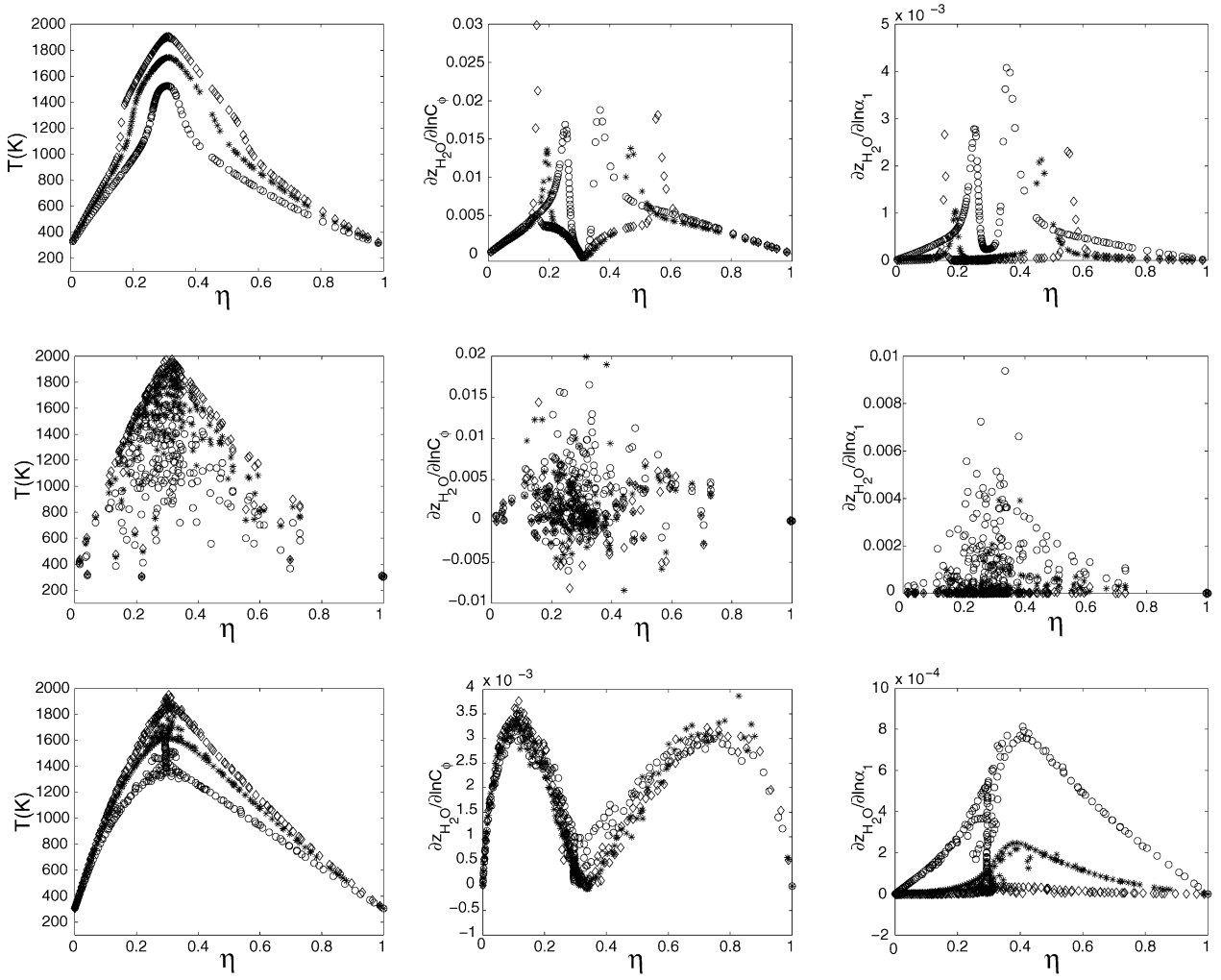

Fig. 8. In the mixture fraction space, scatterplots of temperature T, sensitivities of H_2O to the mixing model constant C_ϕ, and sensitivities of H_2O to the pre-exponential factor α_1 of R1, for different mixing models with different values of τ_{res} and $\tau_t/\tau_{res} = 0.5$. ($\diamond$) $\tau_{res} = 2$ ms; ($*$) $\tau_{res} = 0.3$ ms; ($\circ$) $\tau_{res} = 0.08$ ms. First row: results from the IEM model; second row: results from the MC model; bottom row: results from the EMST model.

cally. Among the three mixing models, for most cases, with the same residence time, the mean and conditional mean (conditioned on stoichiometric mixture fraction) of the major product H_2O obtained from the EMST model is least sensitive to the mixing model constant and the rates of the chain reactions.

5. Conclusions

We develop a method for the accurate and efficient calculation of sensitivities in PDF calculations of turbulent combustion. The evolution equations for the composition and the sensitivities are solved by numerical schemes based on an operator-splitting approach. As discussed in Section 2.3, the efficient calculation of sensitivities in PDF particle methods can be achieved via the use of the storage–retrieval method ISAT [30] (although this is not implemented here).

In the PDF calculation, for each particle the method enables the calculation of the sensitivities to model parameters of interest. These particle-level sensitivities allow one to examine the particles with the largest sensitivities, and the corresponding compositions reveal the sensitive region in the composition space. As demonstrated, sensitivities of mean (and conditional mean) quantities can be extracted from the particle sensitivities via averaging.

The method is demonstrated in the PDF calculation of the oxidation of a diluted H_2/air mixture in a PaSR using different mixing models. It is shown that the method is capable of accurately calculating the sensitivities at the particle level. It is shown that for all the mixing models, the particle sensitivities depend on their corresponding composition's locations in the composition space. However, there are qualitatively different behaviors in both particle composition and particle sensitivities among the different mixing models. For the PaSR test cases investigated, for the IEM model, the most sensitive region (for all the sensitivity parameters considered) lies close to the boundaries of the reaction zone. With the decrease of

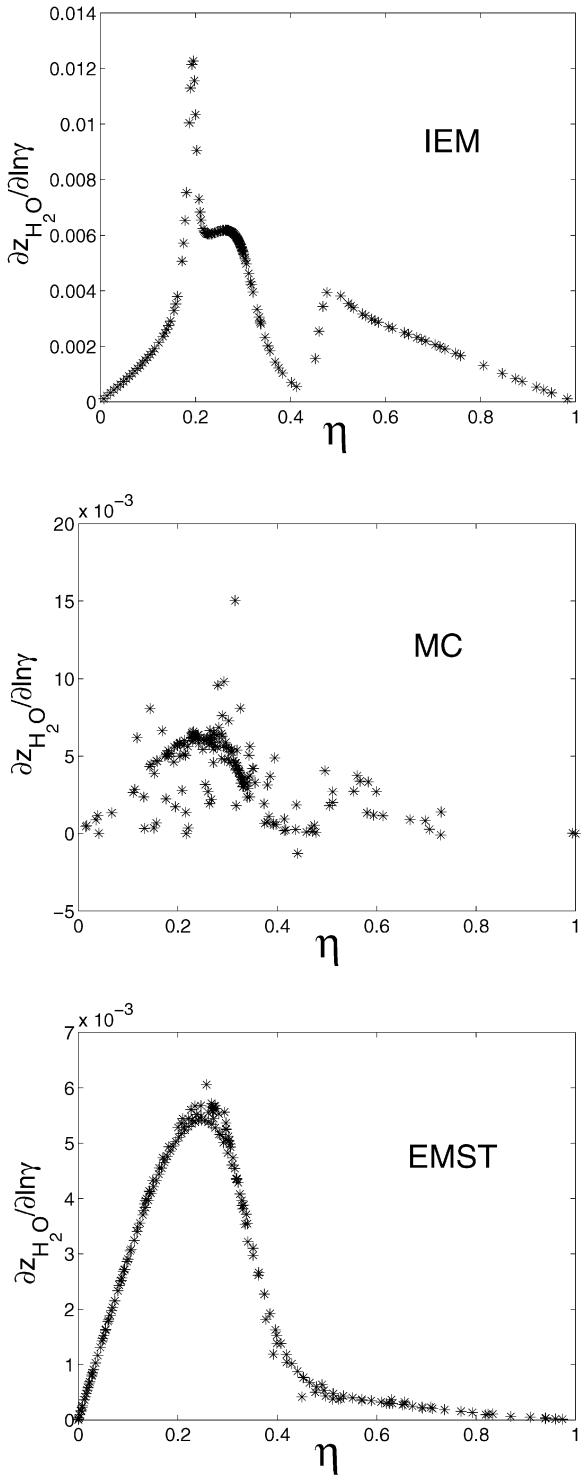

Fig. 9. In the mixture fraction space, scatter plots of sensitivities of H_2O to the hydrogen-to-nitrogen ratio γ of the fuel stream for different mixing models with $\tau_{res} = 0.3$ ms and $\tau_t/\tau_{res} = 0.5$.

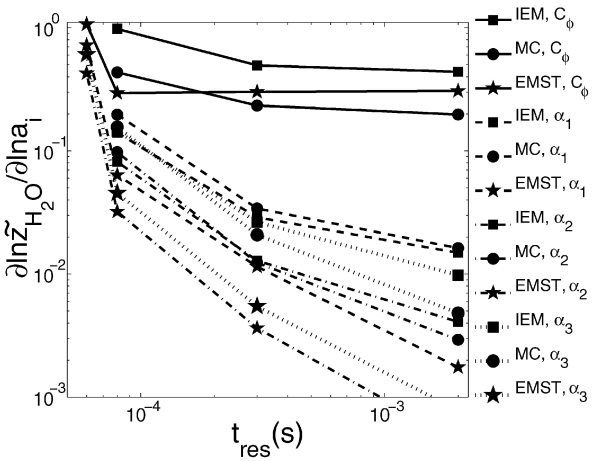

Fig. 10. Sensitivities (to the mixing model constant C_ϕ and the pre-exponential factors of the reactions listed in Eq. (18)) of mean specific moles of H_2O against residence time with $\tau_t/\tau_{res} = 0.5$. Solid line: sensitivities to the mixing model constant C_ϕ; dashed line: sensitivities to the pre-exponential factor of R1; dashed–dotted line: sensitivities to the pre-exponential factor of R2; dotted line: sensitivities to the pre-exponential factor of R3. Lines with solid squares: results from IEM; lines with solid stars: results from MC; lines with solid circles: results from EMST.

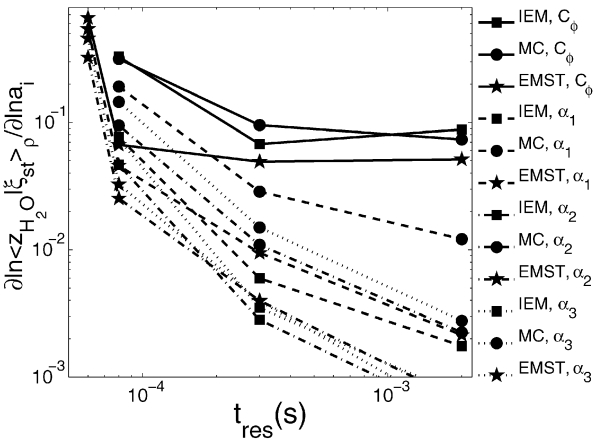

Fig. 11. Sensitivities (to the mixing model constant C_ϕ and the pre-exponential factors of the reactions listed in Eq. (18)) of the conditional mean specific moles of H_2O (conditional on stoichiometric mixture fraction) against residence time with $\tau_t/\tau_{res} = 0.5$. Solid line: sensitivities to the mixing model constant C_ϕ; dashed line: sensitivities to the pre-exponential factor of R1; dashed–dotted line: sensitivities to the pre-exponential factor of R2; dotted line: sensitivities to the pre-exponential factor of R3. Lines with solid squares: results from IEM; lines with solid stars: results from MC; lines with solid circles: results from EMST.

the residence time toward global extinction, the most sensitive region in the composition space moves toward stoichiometry. In contrast, for the EMST model, for a particular sensitivity parameter, the most sensitive region and the shape of the sensitivity distribution in the composition space remain almost the same over a wide range of residence times. However, the most sensitive regions in the composition space are different for different sensitivity parameters. For the MC model, no clear pattern can be observed from the particle-level sensitivities (even to some extent they reveal the most sensitive region). The sensitivities of mean (and conditional mean) quantities confirm that when combustion is controlled by mixing, composi-

tions are insensitive to chemistry. When the reactive system approaches global extinction, the sensitivity of the combustion both to mixing and to chemistry increases (in magnitude) dramatically.

Acknowledgment

This research is supported by the Department of Energy under Grant DE-FG02-90ER.

References

[1] C.T. Bowman, Proc. Combust. Inst. 15 (1974) 869–877.
[2] A.A. Boni, R.C. Penner, Combust. Sci. Technol. 15 (1977) 99–106.
[3] R. Yetter, L.A. Eslava, F.L. Dryer, H. Rabitz, J. Phys. Chem. 88 (1984) 1497–1507.
[4] H. Rabitz, M. Kramer, D. Dacol, Annu. Rev. Phys. Chem. 34 (1983) 419–461.
[5] M.A. Kramer, H. Rabitz, J.M. Calo, R.J. Kee, Int. J. Chem. Kinet. 16 (1984) 559–578.
[6] T. Turányi, J. Math. Chem. 5 (1990) 203–248.
[7] M.R. Mishra, R. Yetter, Y. Reuven, H. Rabitz, M.D. Smooke, Int. J. Chem. Kinet. 26 (1994) 437–453.
[8] R.C. Brown, C.E. Kolb, R.A. Yetter, F.L. Dryer, H. Rabitz, Combust. Flame 101 (1995) 221–238.
[9] Z. Zhao, J. Li, A. Kazakov, F.L. Dryer, Int. J. Chem. Kinet. 37 (2005) 282–295.
[10] A.E. Lutz, R.J. Kee, J.A. Miller, SENKIN: A Fortran program for predicting homogeneous gas phase chemical kinetics with sensitivity analysis, Technical Report SAND87-8248, Sandia National Laboratories, 1987.
[11] R.J. Kee, F.M. Rupley, E. Meeks, J.A. Miller, CHEMKIN-III: A FORTRAN chemical kinetics package for the analysis of gas-phase chemical and plasma kinetics, Sandia Report SAND96-8216, Sandia National Laboratories, Livermore, CA, 1996.
[12] CANTERA: Objected-oriented software for reacting flows, http://www.cantera.org/.
[13] S.B. Pope, Prog. Energy Combust. Sci. 11 (1985) 119–192.
[14] Q. Tang, J. Xu, S.B. Pope, Proc. Combust. Inst. 28 (2000) 133–139.
[15] R. Cao, S.B. Pope, A.R. Masri, Combust. Flame 142 (2005) 438–453.
[16] A.R. Masri, R. Cao, S.B. Pope, G.M. Goldin, Combust. Theory Model. 8 (2004) 1–22.
[17] J. Xu, S.B. Pope, Combust. Flame 123 (2000) 281–307.
[18] R.P. Lindstedt, S.A. Louloudi, E.M. Váos, Proc. Combust. Inst. 28 (2000) 149–156.
[19] R. Cao, H. Wang, S.B. Pope, Proc. Combust. Inst. 31 (2007) 1543–1550.
[20] J. Villermaux, J.C. Devillon, in: Proceedings of the 2nd International Symposium on Chemical Reaction Engineering, Elsevier, New York, 1972.
[21] C. Dopazo, E.E. O'Brien, Acta Astronaut. 1 (1974) 1239–1266.
[22] J. Janicka, W. Kolbe, W. Kollman, J. Nonequilib. Thermodynam. 4 (1979) 47–66.
[23] S. Subramaniam, S.B. Pope, Combust. Flame 115 (1998) 487–514.
[24] Z. Ren, S. Subramaniam, S.B. Pope, Implementation of the EMST mixing model, http://eccentric.mae.cornell.edu/~tcg/emst/.
[25] ADIFOR 2.0, Automatic differentiation of Fortran, http://www-unix.mcs.anl.gov/autodiff/ADIFOR/.
[26] G.I. Marchuk, On the theory of the splitting-up method, in: Proceedings of the 2nd Symposium on Numerical Solution of Partial Differential Equations, SVNSPADE, 1970, pp. 469–500.
[27] N.N. Yanenko, in: M. Holt (Ed.), The Method of Fractional Steps, Springer-Verlag, New York, 1971.
[28] G. Strang, SIAM J. Numer. Anal. 5 (3) (1968) 506–517.
[29] M. Caracotsios, W.E. Stewart, Comput. Chem. Eng. 9 (4) (1985) 359–365.
[30] S.B. Pope, Combust. Theory Model. 1 (1997) 41–63.
[31] S.M. Correa, Combust. Flame 93 (1993) 41–60.
[32] J.-Y. Chen, Combust. Sci. Technol. 122 (1997) 63–94.
[33] B. Yang, S.B. Pope, Combust. Flame 112 (1998) 16–32.
[34] Z. Ren, S.B. Pope, Combust. Flame 136 (2004) 208–216.
[35] U. Maas, J. Warnatz, Proc. Combust. Inst. 22 (1988) 1695–1704.